NASA Technical Paper 1116

Simulator Evaluation of a Flight-Path-Angle Control System for a Transport Airplane With Direct Lift Control

Wendell W. Kelley

MARCH 1978

NASA

NASA Technical Paper 1116

Simulator Evaluation of a Flight-Path-Angle Control System for a Transport Airplane With Direct Lift Control

Wendell W. Kelley
Langley Research Center
Hampton, Virginia

NASA
National Aeronautics and Space Administration

Scientific and Technical Information Office

1978

SUMMARY

A piloted simulator was used to evaluate the flight-path-angle control capabilities of a system that employs spoiler direct lift control. This system was designated the Velocity Vector Control System and was compared with a baseline flight-path-angle control system which used elevator for control. The simulated airplane was a medium jet transport that is used as a research vehicle by the National Aeronautics and Space Administration (NASA). Research pilots flew a manual instrument landing system glide-slope tracking task and a variable flight-path-angle task in the landing configuration to obtain comparative performance data.

Results of the study showed that the Velocity Vector Control System provided a very responsive and stable flight-path-angle rate command system. Flight-path-angle stability in the presence of wind disturbances was excellent. The baseline system exhibited comparatively sluggish response to short-term flight-path-angle control requirements and was less stable in wind disturbances. Also, the use of Velocity Vector Control System resulted in less pitch-angle, angle-of-attack, and normal-acceleration activity in the presence of turbulence.

INTRODUCTION

Precise control of airplane flight-path angle γ is an important task during many phases of flight. This is especially true in the terminal area where maneuvers such as the landing approach are often made difficult by adverse wind conditions. As a part of the Langley Research Center's Terminal Configured Vehicle Program, a system designed to enhance flight-path-angle control in piloted modes has previously been flight tested on the research airplane shown in figure 1, and the results are reported in reference 1. That system, which is designated the "baseline system" in this study, used elevator for flight-path-angle control. The pilot controlled γ by manipulating pitch controls and by reference to a display on the cockpit electronic attitude director indicator. Comments from the pilots that had experience with the baseline system generally indicated a desire for quicker flight-path-angle response and better control precision, especially in turbulence and wind shears.

As a result of investigations into ways of providing the desired control improvements, a new system called the Velocity Vector Control System was developed and tested by using ground-based simulation. The design of the Velocity Vector Control System was based on the use of spoiler direct lift control which provided a more rapid lift modulation than could be produced by using the airplane elevator system. Pilot display and control functions remained the same as for the baseline system. This report presents results of the piloted simulator study which was used to evaluate the performance of the two systems during selected flight-path-angle control tasks. Flight characteristics of the research airplane in the landing configuration were used in the simulation study. Appendix A and table I contain a brief description of the physical characteristics of the airplane.

SYMBOLS AND ABBREVIATIONS

Values are presented in both SI and U.S. Customary Units. Calculations were made in U.S. Customary Units.

ADEDS advanced electronic display system

AFD aft flight deck

DLC direct lift control

EADI electronic attitude director indicator

EHSI electronic horizontal situation indicator

EPR engine pressure ratio

FFD forward flight deck

g acceleration due to gravity, 9.81 m/sec^2 (32.2 ft/sec^2)

$\dot{h}$ vertical velocity (climbing, positive), m/sec (ft/sec)

$\ddot{h}$ vertical acceleration (upward, positive), m/sec^2 (ft/sec^2)

I_{XX} moment of inertia about body X axis, kg-m^2 (slug-ft^2)

I_{YY} moment of inertia about body Y axis, kg-m^2 (slug-ft^2)

I_{ZZ} moment of inertia about body Z axis, kg-m^2 (slug-ft^2)

I_{XZ} product of inertia about body X and Z axes, kg-m^2 (slug-ft^2)

ILS instrument landing system

MLS microwave landing system

MSL mean sea level

NCDU navigation control and display unit

n_Z normal acceleration (up, positive), g units

PMC panel-mounted controller

PMC pitch panel-mounted controller position forward or aft of neutral (aft, positive), cm (in.)

rms	root mean square
s	Laplace variable
TCV	terminal configured vehicle
VVCS	Velocity Vector Control System
α	airplane fuselage reference line angle of attack, deg
γ	flight-path angle; angle between airplane inertial velocity vector (Earth referenced) and local horizontal reference plane (climbing, positive), deg
$\dot{\gamma}$	rate of change of flight-path angle (upward, positive), deg/sec
γ_c	pilot-commanded flight-path angle (climbing, positive), deg
γ_T	flight-path-angle profile defined by the tracking task (climbing, positive), deg
ΔSP	change in spoiler position due to direct lift control; measured relative to spoiler bias position (up positive), deg
ΔSP_c	spoiler command for direct lift control (up, positive), deg
$\Delta\gamma$	flight-path-angle error signal (climbing, positive), deg
$\Delta\theta$	change in pitch angle from level flight trim value (nose up, positive), deg
δ_e	elevator position (trailing edge down, positive), deg
δ_{ec}	command to elevator power control unit (trailing edge down, positive), deg
δ_{sp}	total spoiler position due to direct lift control and speed-brake handle inputs (all values positive), deg
θ	pitch angle (nose up, positive), deg
$\dot{\theta}$	pitch rate (nose up, positive), deg/sec
ϕ	roll angle (right wing down, positive), deg

PROBLEM BACKGROUND

Design details of the baseline and Velocity Vector Control System (VVCS) control laws are included in appendixes B and C, respectively. The common design goal of each was to provide stability and control augmentation to assist the pilot in flying a desired flight-path angle. However, the method of achieving this goal differs somewhat in each case due to the control systems which were used. Therefore, a brief analysis is included herein to point out response characteristics of the test airplane due to elevator and spoiler control inputs.

The baseline system uses elevator to control γ. Simulated airplane responses are shown in figure 2 for various magnitudes of elevator input. Note that for each deflection of the elevator there is an initial wrong-way acceleration of the airplane. This reaction is due to tail downloads that are required to generate additional angle of attack α for increased lift. Also note that delays on the order of 1 sec occur before appreciable changes in γ are obtained. These characteristics indicate potential problems with the use of elevator systems for flight-path-angle control when rapid response is required.

The VVCS design utilizes spoiler direct lift control (DLC) to overcome the lags in the γ response noted above. Figure 2 shows the results of activating spoiler controls. Since wing lift is affected almost immediately by changes in spoiler deflection, there is essentially no delay between spoiler control application and airplane acceleration in the desired direction. Note, however, that an adverse pitching moment due to spoiler aerodynamics tends to override the favorable lift effects of DLC after approximately 1 sec. To counteract this effect, VVCS uses elevator to cancel the adverse pitching moment and thereby achieves both short-term and long-term beneficial lift effects. The combined elevator and spoiler inputs are also shown in figure 2. Thus, VVCS uses spoilers for high-frequency response to initiate γ changes and elevator for attitude control and stabilization.

EXPERIMENTAL EQUIPMENT

Simulator

The simulator is designed to provide realistic simulation of the NASA research airplane shown in figure 1. In addition to the normal pilot stations, the airplane is equipped with a research cockpit that is designated the "aft flight deck" (AFD) and is located behind the front cockpit.

The simulator is designed to duplicate the full range of airplane operation from the AFD. The fixed base system is driven by a high-speed digital computer complex which updates the simulation model at the rate of 32 iterations/sec. The simulation model includes nonlinear aerodynamic data which were derived from both flight and wind-tunnel tests. The six degree-of-freedom equations of motion include round-Earth effects. Also included are turbulence and wind-shear models with variable parameters. Flight-control system models account for all known hysteresis, deadbands, or other nonlinearities in the actuating mechanisms.

Cockpit Arrangement

Figure 3 shows details of the simulator cockpit. Rudder pedals, throttles, the flap lever, and the speed-brake handle are all conventionally designed controls. However, each control column is replaced by a set of pitch and roll controllers mounted on the instrument panel and referred to as panel-mounted controllers (PMC). The PMC consists of cylinders which slide fore and aft for longitudinal control and rotate about the cylindrical axis for lateral control. The pitch-control force gradient is 14 N/cm (8.0 lb/in.) with a 17-N (4.0-lb) breakout force. Handgrips with standard control column switches are attached to the cylinders.

The advanced electronic display system (ADEDS) is an integral part of most research and development efforts conducted on both the simulator and the airplane. The ADEDS is an integrated navigation, guidance, and display system based on a design developed for the Boeing supersonic transport prototype program. A detailed description of the ADEDS system is contained in references 2 and 3.

The electronic attitude director indicator (EADI) and electronic horizontal situation indicator (EHSI) are primary displays used for airplane navigation and control. A navigation control and display unit (NCDU) provides for flexible automatic navigation functions.

The 20-cm (8-in.) EADI (fig. 4) was the primary display instrument used in this study. The horizon line, pitch scale, and airplane symbol provide pitch-angle information. A roll pointer and bank-angle index at the top of the display provide roll angle. Pilot-commanded flight-path angle γ_c is displayed by a set of wedge-shaped symbols and is referenced to the horizon line. Actual γ is displayed by a set of rectangular bars located adjacent to the γ_c wedges.

The small dashed-line symbol (pitch reference line) may be driven automatically or set by the pilot to any angle above or below the horizontal line. Glide-slope and localizer deviation scales are available for ILS or MLS approaches. Radar altitude is displayed in the upper right-hand corner of the screen, and conventional round instruments were used for indicated airspeed, barometric altitude, and vertical velocity.

RESULTS AND DISCUSSION

Flight-Path-Angle Rate Tests

Simulated airplane responses with the VVCS and the baseline system were obtained for step inputs at the pilot PMC controls (fig. 5). The long-term result of a step PMC input with either system is to establish a rate of change of flight-path angle $\dot{\gamma}$ whose magnitude depends upon airspeed and the size of the input. However, the short-term response is of greater importance for tasks which involve frequent γ changes. The $\dot{\gamma}$ response for the VVCS case was rapid and very stable. The airplane accelerated very smoothly to a steady-state value of $\dot{\gamma}$ and no overshoot occurred. Comparatively, the baseline system exhibited much less stability, as can also be seen in figure 5. After a momentary acceleration in the wrong direction, a $\dot{\gamma}$ overshoot of approximately 55 percent occurred, followed by a lightly damped oscillation.

ILS Tracking Task

A research pilot with flying experience in the test airplane was used to gather tracking performance data for an ILS approach task. The primary objective was to compare γ control performance with the VVCS and baseline system during a 3° glide-slope intercept and tracking task. Additionally, objectives were to compare airplane pitch-angle θ and α activity, as well as normal-acceleration n_z response in turbulence. A Dryden model was used to simulate 0.30 m/sec (1 ft/sec) root-mean-square (rms) turbulence on the approaches.

Flight conditions for the tests are listed in table II. Each run began with the airplane trimmed in level flight on the ILS localizer approximately one dot below the glide slope. The pilot was instructed to maintain airspeed while tracking the glide slope as closely as possible. Raw glide-slope deviation information was the only cue for vertical error. Glide-slope tracking continued down to an altitude of 15 m (50 ft) where the task was terminated. Localizer errors were ignored.

Several approaches were flown with each control configuration. However, due to the large amount of recorded data, it was not convenient to present time histories of each run. Therefore, figure 6 shows time histories of a typical run with the VVCS and baseline system. Note that as the airplane approached the glide slope, the pilot applied controls so as to cause the commanded γ to change from 0° (level flight) to -3°. The manner in which he did this is fairly consistent for both runs. However, airplane response to the γ command was significantly different for the two systems. First, note that there was a considerable overshoot in γ for the baseline system and a noticeable oscillation about the commanded γ (-3°). These oscillations continued throughout the approach even though a period of 55 sec existed during which no control inputs were applied. To aid in the analysis, the quantity $\gamma_c - \gamma$ (the γ error signal) is also plotted. Flight-path-angle errors up to $\pm 0.4^\circ$ were typical throughout the baseline approach.

Next, note the results of an identical approach with the Velocity Vector Control System. Inspection of the $\gamma_c - \gamma$ trace shows that the airplane followed pilot commands very closely and that the turbulence which degraded the stability of the baseline system had practically no effect on VVCS. The result was a smoother, more stable approach which permitted the pilot to select a desired γ and to rely upon the system stability to hold that flight-path angle without further pilot assistance. Note that the error in γ rarely exceeded $\pm 0.1^\circ$ and was usually $\pm 0.05^\circ$ or less.

Other by-products of the Velocity Vector Control System were reduced θ and α activity and lower levels of n_z. (See fig. 6.) These by-products are a result of the fact that the baseline system used θ and α to generate the necessary lift modulation, whereas the VVCS employed spoilers to achieve the same result.

After the initial maneuver to intercept the glide slope with VVCS, n_z deviations from 1.00 rarely exceeded ±0.01g and were usually below that value. The baseline system, on the other hand, experienced n_z excursions of up to ±0.05g throughout the approach. This translates into an 80-percent reduction in airplane reaction to turbulence with VVCS and indicates a sizable potential for improving passenger ride comfort.

Variable Flight-Path-Angle Tracking Task

Another NASA research pilot was used to gather data during a variable flight-path-angle tracking task. The objective was to determine capabilities of both control systems in an environment that involves frequent γ changes. Flight conditions for this task were identical to the ILS approach task except the initial flight-path angle, which was -1°. The pilot was instructed to follow a computer-generated γ_T profile (target) which was displayed on the dotted pitch reference line on the EADI (fig. 4). The reference line was driven by the computer so that it moved up and down the pitch scale of the EADI according to the time profile shown in figure 7. The profile variations in γ_T (-3.5° to 4.0°) were considered typical for maneuvering in the terminal approach and go-around flight phases.

As the target line moved according to the profile, the pilot applied PMC pitch control so as to make the γ_c wedges follow the line as closely as possible. Task objectives were ideally more suited to an automatic procedure (pilot not in the loop), but such a procedure was not available at the time of the test. Rate of movement of the target line was approximately 0.25 deg/sec. The pilot commented that he had no trouble keeping up with this rate and that fatigue was not a factor. Several practice runs were completed before the pilot stated that he was familiar with the task requirements and accustomed to the control forces required. No turbulence or wind shears were included. Speed was maintained by the autothrottle system.

Results of the γ tracking task are shown for the Velocity Vector Control System in figure 8 and for the baseline system in figure 9. Since the objective of the task was primarily to determine airplane performance rather than pilot performance, it was first necessary to compare pilot inputs for the VVCS and baseline system. Note that pilot inputs for both systems followed the task profile very closely and were similar enough to be considered practically identical.

Airplane flight-path-angle performance is easily seen by inspection of the γ_c, γ, and $\gamma_c - \gamma$ traces. The VVCS was very responsive to pilot inputs and tracked γ_c closely throughout the task. This is most apparent in the $\gamma_c - \gamma$ trace. Airplane flight-path-angle errors never exceeded $\pm 0.2^{\circ}$ during the ramp changes in γ_T and reached a maximum magnitude of 0.5° only after the pilot's attempt to follow a step change in γ_T. The γ trace verifies that the path of the airplane very closely matched the task profile. Pitch-angle activity was minimized since changes in θ were only necessary to satisfy long-term trim requirements as the steady-state value of γ changed.

The baseline system was less responsive and less stable by comparison. Figure 9 shows that γ errors were typically $\pm 0.5^\circ$ during the ramp changes in γ_T and were as large as 1.3° during the step changes. Pitch-angle activity was also somewhat higher for the baseline system; this was an expected result since elevator-generated α was needed to perform the changes in γ.

Notable differences in α activity were seen for the two systems. Again, the baseline system depends heavily on α modulation whereas the VVCS operates at fairly constant values of α and uses spoilers for lift modulation.

CONCLUSIONS

A piloted simulator was used to evaluate the performance capabilities of two flight-path-angle control systems for a medium jet transport. A baseline system that used elevator for flight-path-angle control was compared with a Velocity Vector Control System which utilized spoiler direct lift control. Research pilots flew an instrument landing system glide-slope tracking task and a variable flight-path-angle task with the airplane in final approach configuration. Based upon simulator results, the following conclusions were drawn:

1. For the simulated transport airplane, use of spoiler direct lift control provided better flight-path-angle response capability than elevator control. Adverse spoiler pitching moment was easily canceled by elevator control without significantly affecting the favorable spoiler lift effects. In this study, the Velocity Vector Control System provided a very responsive and stable flight-path-angle rate command system. The baseline control system was less responsive by comparison and exhibited a lightly damped flight-path-angle rate control response.

2. Flight-path-angle stability was much better for the Velocity Vector Control System during the 3° instrument landing system glide-slope tracking task. The airplane maintained flight-path angle within $\pm 0.1^\circ$ of pilot commands throughout an approach which included turbulence. The baseline system produced flight-path-angle errors that were larger by a factor of 4.

3. In an environment of frequent flight-path-angle changes, the Velocity Vector Control System displayed response and stability advantages. A flight-path-angle tracking task resulted in nominal flight-path-angle errors of $\pm 0.2^\circ$ for the Velocity Vector Control System and $\pm 0.5^\circ$ for the baseline system.

4. Airplane pitch-angle and angle-of-attack activity was reduced with the Velocity Vector Control System, primarily due to spoiler direct lift control.

5. Normal accelerations encountered with the Velocity Vector Control System during turbulence were 80 percent less than those of the baseline system and offered a definite potential for improving passenger ride comfort.

Langley Research Center
National Aeronautics and Space Administration
Hampton, VA 23665
December 13, 1977

APPENDIX A

RESEARCH AIRPLANE

The research airplane, operated by the Langley Research Center, is a twin-engine medium jet transport that was modified to include an advanced research cockpit and onboard flight research equipment. A cutaway view of the airplane is shown as figure 1. Equipped with triple-slotted trailing-edge flaps, leading-edge slats, and Krueger leading-edge flaps, the vehicle was designed for medium- and short-haul operations into smaller airports with limited runway length. Longitudinal control is achieved by an elevator and movable stabilizer, and lateral control is obtained by combined aileron and spoilers. A single-surface rudder provides directional control. The two turbofan engines are equipped with deflector doors for reverse thrust operation.

Figure 10 shows details of the wing spoiler arrangement. Spoiler panels 2, 3, 6, and 7 are flight spoilers which may be deployed in flight by actuating the speed-brake handle. These four spoiler panels were used for the DLC simulation discussed in this report. All eight spoiler panels may be deployed on the ground to reduce stopping distance.

The airplane has two cockpits equipped with pilot controls and displays. The forward cockpit, designated the "forward flight deck" (FFD), was modified to allow transfer of control to and from the aft-located research cockpit. The FFD is used primarily as a safety pilot station during research flight operations.

Most of the research activities are centered around the aft flight deck (AFD), which is located in the forward portion of the passenger compartment. The AFD contains a complete two-man pilot station equipped with advanced displays and fly-by-wire controls. Control commands are processed by a triplex digital flight-control computer system and transmitted to the various hydraulic units which power the control surfaces. When the AFD is in control, FFD controls are back driven so that they continuously follow up the control-surface positions commanded from the AFD.

APPENDIX B

DESCRIPTION OF THE BASELINE-SYSTEM CONTROL LAW

As a result of the VVCS development effort, it was recognized that further optimization of the baseline system could be achieved by refinements to the control law. However, the existing baseline design was used as a basis of comparison in this study.

Figure 11 shows a functional schematic of the baseline-system control law. Pilot inputs on the PMC are used in two separate paths to effect elevator commands. The path designated as 1 is a "feed-forward" path which provides a direct elevator command to quickly start the airplane pitching in the appropriate direction for the desired change in γ. This signal is summed with others to form the signal designated 7 which, after appropriate scaling, becomes the elevator command (δ_{ec}).

The second path for PMC inputs is integrated to form the commanded flight-path angle γ_c shown as path 2. Combining this reference signal with the actual γ signal 3 results in the error signal $\Delta\gamma$, which is then used to drive the elevator as necessary to hold γ. (Actual γ is derived by a computation in the flight-control computers which uses $\dot{h}$ and ground speed.)

Inner-loop stabilization is provided by two paths. The primary stabilization signal is the $\delta_{ec}/\Delta\gamma$ gain shown as path 4. To avoid steady-state standoff errors which would occur due to bias error signals or elevator trim requirements, an integral path 5 was also added. (A pitch trim change which must be canceled by the elevator would otherwise cause a steady-state error.)

Short-period mode damping is provided by pitch-rate feedback 6. Roll-angle feedback is used to cancel a loss of the vertical component of lift due to bank angles.

APPENDIX C

DESCRIPTION OF THE VELOCITY-VECTOR-CONTROL-SYSTEM CONTROL LAW

Figure 12 is a schematic diagram of the VVCS control law. Three separate feed-forward paths are used for open-loop control. As in the baseline system, PMC signals are sent through a gain and noise filter along path 1 to initiate pitch response through the elevator. The VVCS also sends this PMC signal along path 2 directly to the spoilers to provide an immediate lift increment to start changing γ. Finally, to counteract spoiler pitching moment, the spoiler command signal is crossfed to provide additional elevator control along path 3.

The closed-loop error signal $\Delta\gamma$ is formed identically to that of the baseline system. Pilot commands 4 are integrated to form γ_c, which is then compared with γ to form the error signal.

Closed-loop stability and control is accomplished by combining elevator and spoiler control. The primary elevator stabilization signal is derived from passing the $\Delta\gamma$ signal through a high-gain lead-lag filter 5. An integral path 6 was added to take care of possible standoff errors of the type mentioned in appendix B. Spoiler closed-loop control provides rapid lift modulation for precise γ stability in the presence of turbulence and wind shears. Vertical acceleration feedback 7 essentially provides a $\dot{\gamma}$ signal for stabilization and $\Delta\gamma$ 8 provides long-term spoiler corrections for flight-path-angle errors.

Another design feature of the VVCS is its use of EPR feedback for canceling pitching moment due to thrust changes. The technique is based upon knowledge of the relationship between engine location, engine thrust, EPR, and elevator effectiveness. An analysis of these factors produced a gain of 8.2 which, when applied to the EPR feedback signal 9, commands the proper amount of elevator to cancel thrust-induced pitching moments. Two benefits are immediately available from this scheme: The pitch activity due to thrust changes is canceled, and an elevator bias signal is provided downstream of the washout integrator 6, allowing a reduction in the integrator gain and thereby contributing to an increase in system stability.

Pitch-rate feedback 10 is used for short-period mode damping. Roll-angle feedback is used to cancel a loss of the vertical component of lift due to bank angles.

REFERENCES

1. Morello, Samuel A.; Knox, Charles E.; and Steinmetz, George G.: Flight-Test Evaluation of Two Electronic Display Formats for Approach to Landing Under Instrument Conditions. NASA TP-1085, 1977.

2. Steinmetz, George G.; Morello, Samuel A.; Knox, Charles E.; and Person, Lee H., Jr.: A Piloted-Simulation Evaluation of Two Electronic Display Formats for Approach and Landing. NASA TN D-8183, 1976.

3. Salmirs, Seymour; and Tobie, Harold N.: Electronic Displays and Digital Automatic Control in Advanced Terminal Area Operations. AIAA Paper No. 74-27, Jan.-Feb. 1974.

TABLE I.- TEST AIRPLANE DIMENSION AND DESIGN DATA

General:	
Overall length, m (ft)	28.65 (94.0)
Height to top of vertical fin, m (ft)	11.28 (37.0)
Typical landing weight, N (lb)	371 400 (83 500)
Wing:	
Area, m^2 (ft^2)	91.04 (980)
Span, m (ft)	28.35 (93.0)
Mean aerodynamic chord, m (ft)	3.41 (11.2)
Aspect ratio	8.83
Sweep of quarter-chord, deg	25
Flap deflection (maximum), deg	40
Inboard ground spoilers (maximum deflection), deg	60
All other spoilers (maximum deflection), deg	40
Horizontal tail:	
Total area, m^2 (ft^2)	28.99 (312)
Span, m (ft)	10.97 (36)
Stabilizer deflection (maximum), deg	-14, +3
Elevator deflection (maximum), deg	±21
Propulsion system (two turbofan engines):	
Maximum uninstalled thrust per engine (sea level static), N (lb)	62 300 (14 000)

TABLE II.- SIMULATION FLIGHT CONDITIONS

Weight, N (lb)	371 400 (83 500)
I_{XX}, kg-m^2 (slug-ft^2)	549 000 (405 000)
I_{YY}, kg-m^2 (slug-ft^2)	1 080 000 (797 000)
I_{ZZ}, kg-m^2 (slug-ft^2)	1 710 000 (1 260 000)
I_{XZ}, kg-m^2 (slug-ft^2)	70 800 (52 200)
Center of gravity, percent of mean aerodynamic chord	19
Initial altitude (MSL), m (ft)	365.8 (1200)
Field elevation (MSL), m (ft)	2 (7)
Indicated airspeed, knots	130
Initial flight-path angle, deg	0
Trailing-edge flap position, deg	40
Flight spoiler position, deg	8
Speed-brake handle position, deg	17.4
Landing-gear position	Down

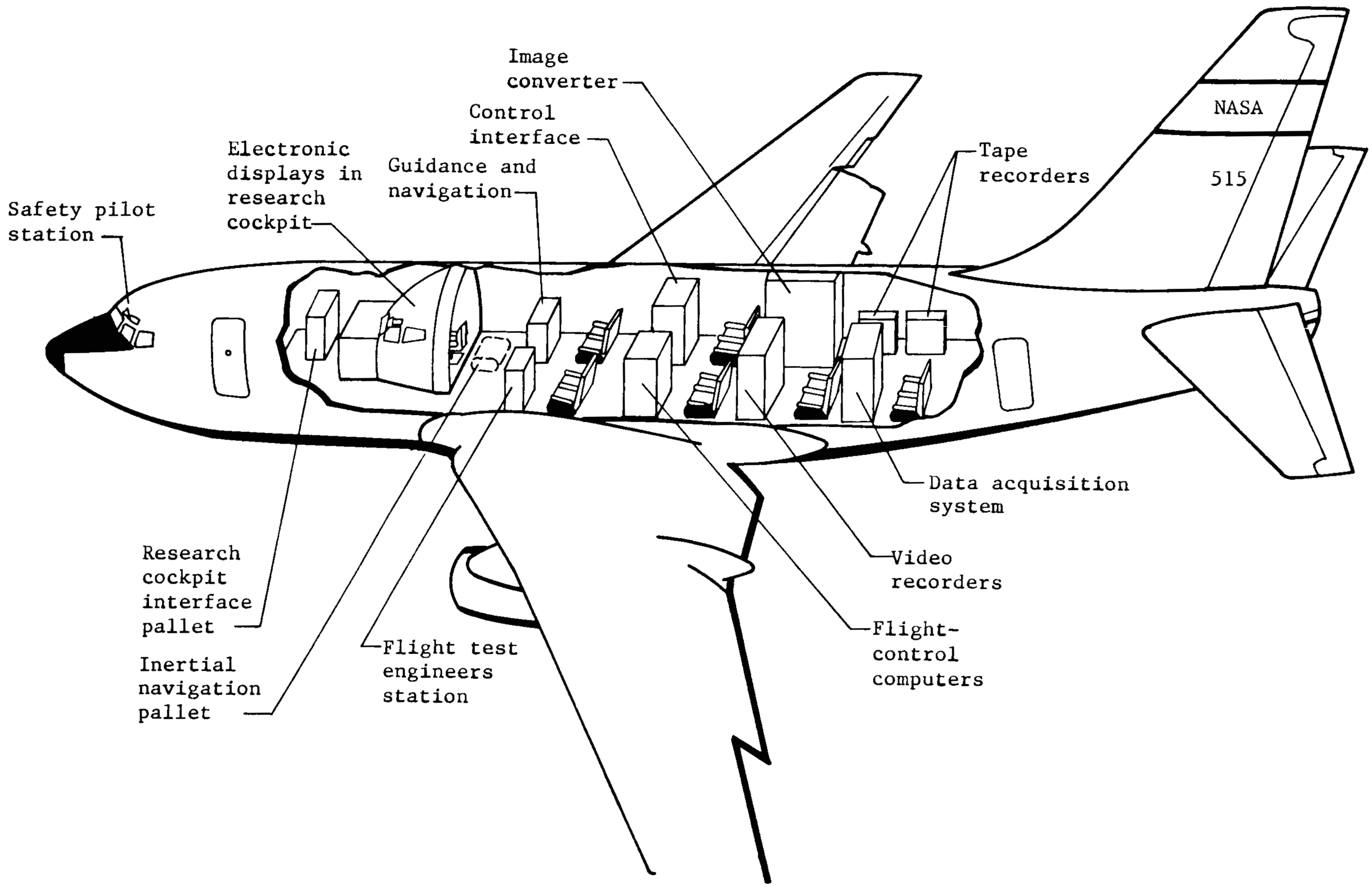

Figure 1.- Internal arrangement of research airplane.

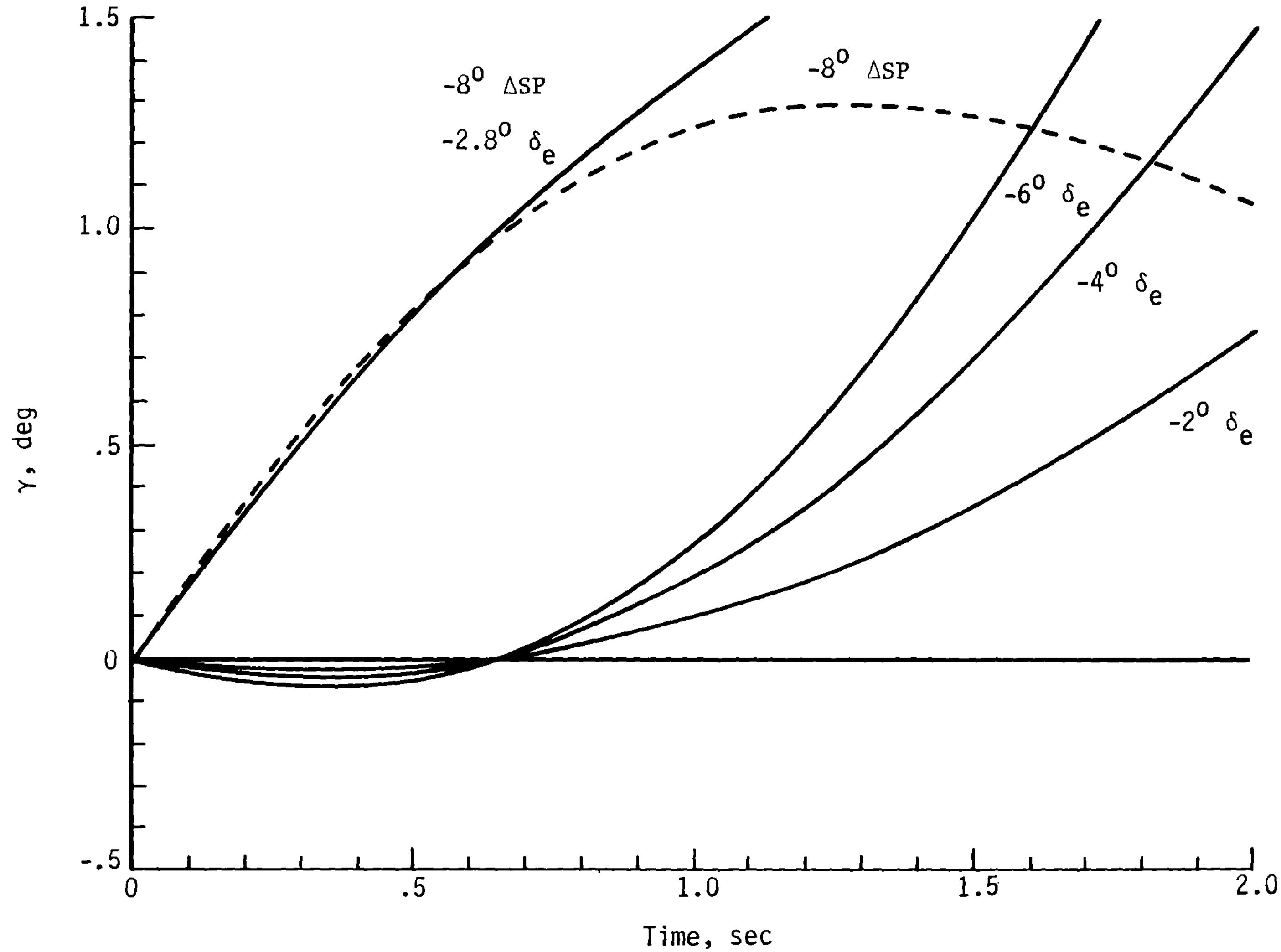

Figure 2.- Simulated test airplane response to step control surface inputs. See table II for flight conditions.

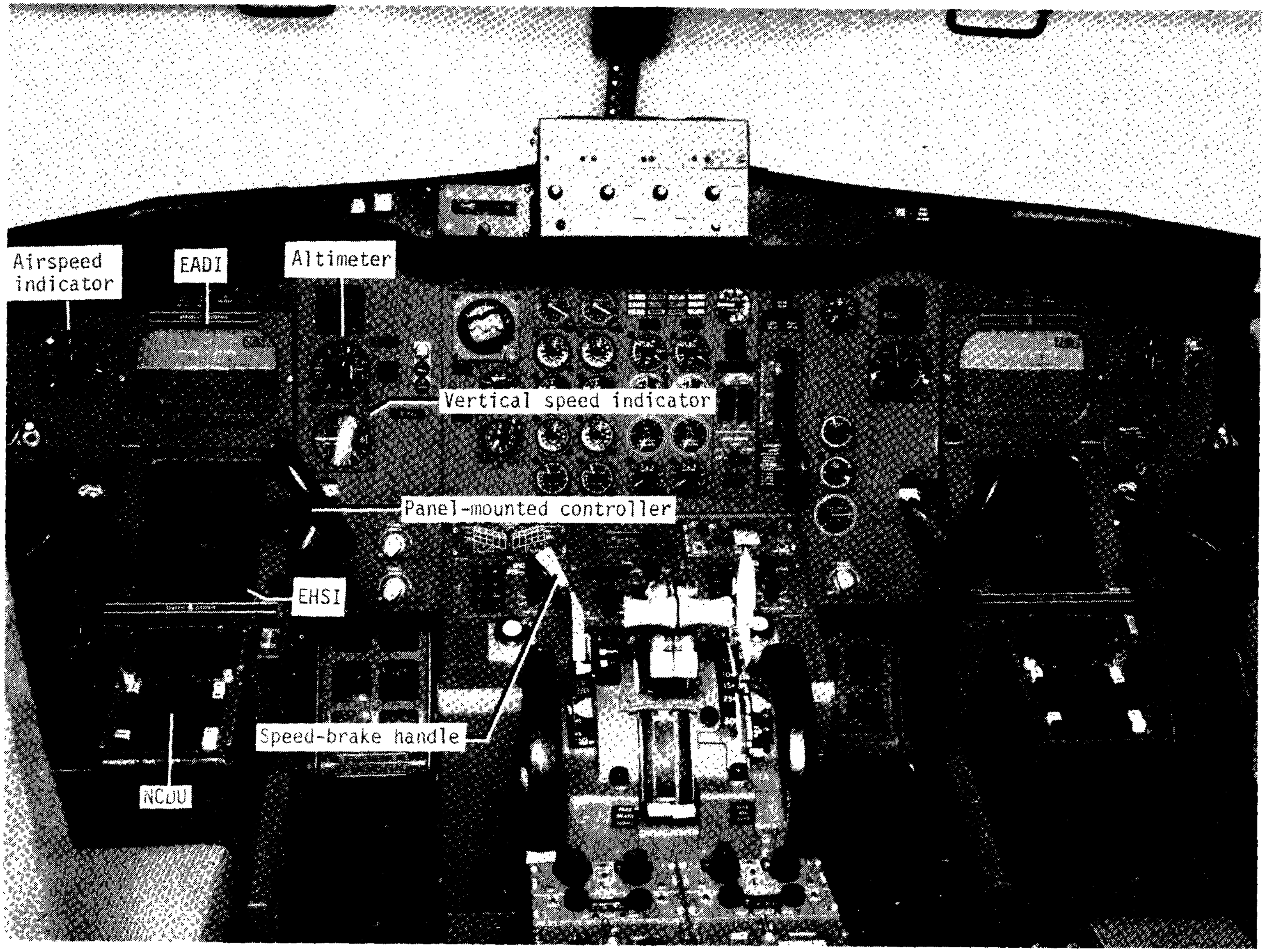

L-74-5183.2

Figure 3.- Simulator cockpit arrangement.

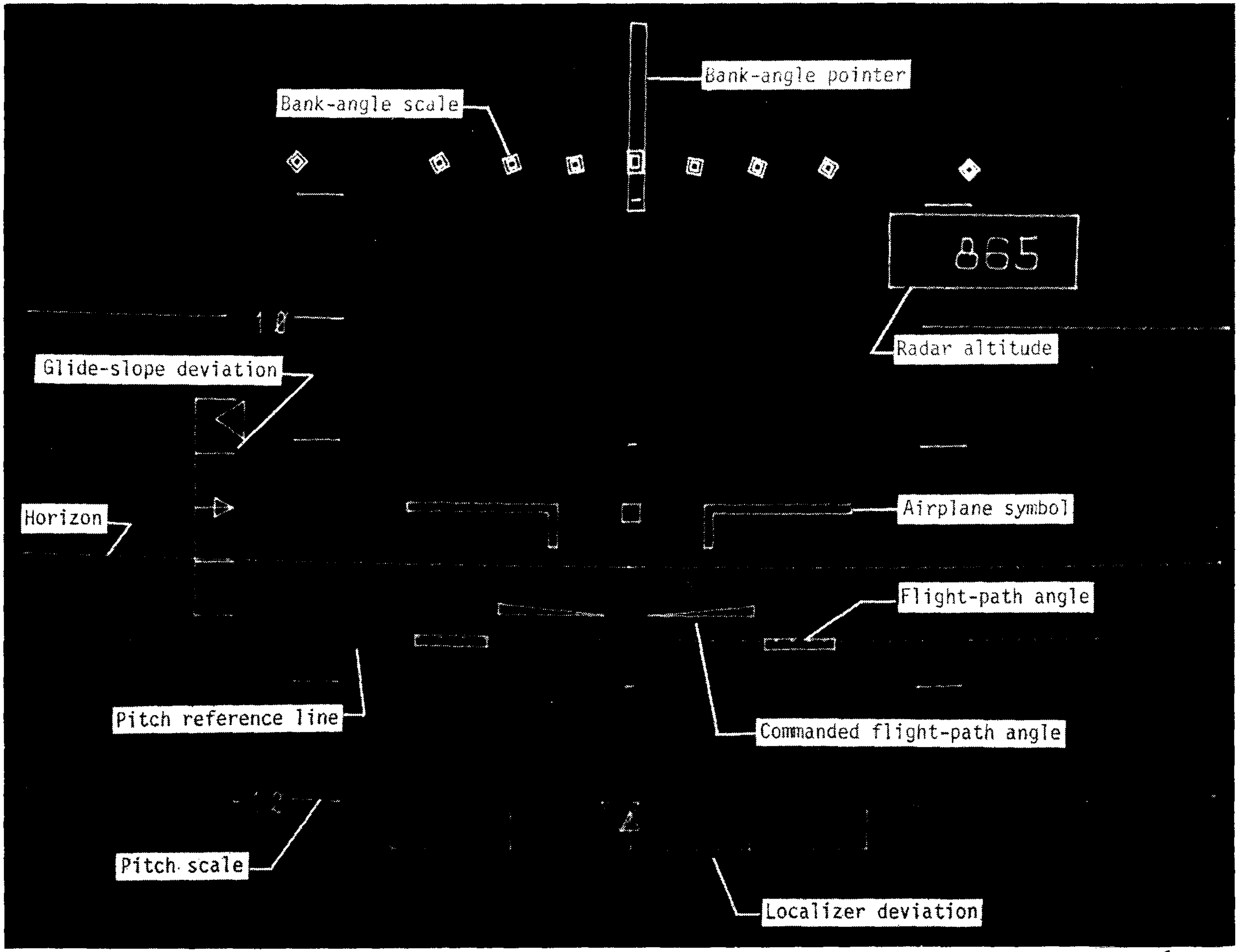

L-77-6352.1

Figure 4.- EADI display.

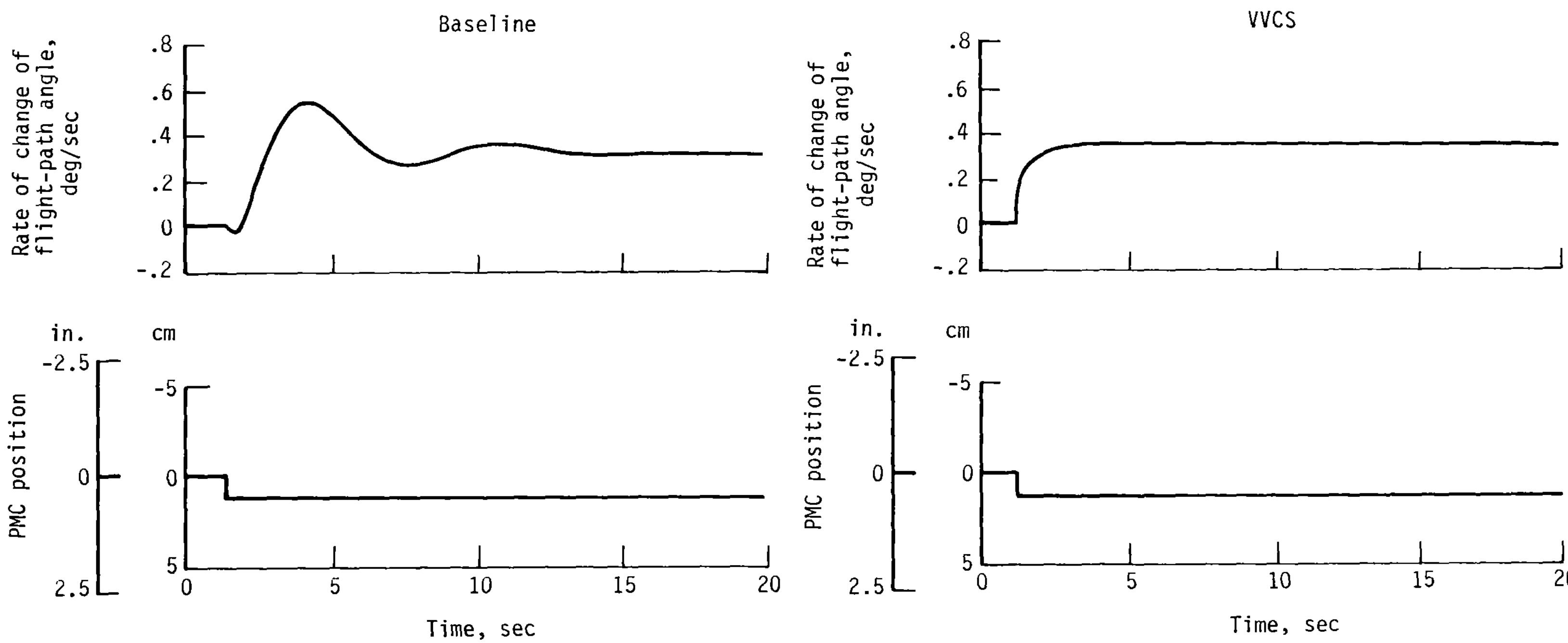

Figure 5.- The $\dot{\gamma}$ response to step PMC inputs. See table II for flight conditions.

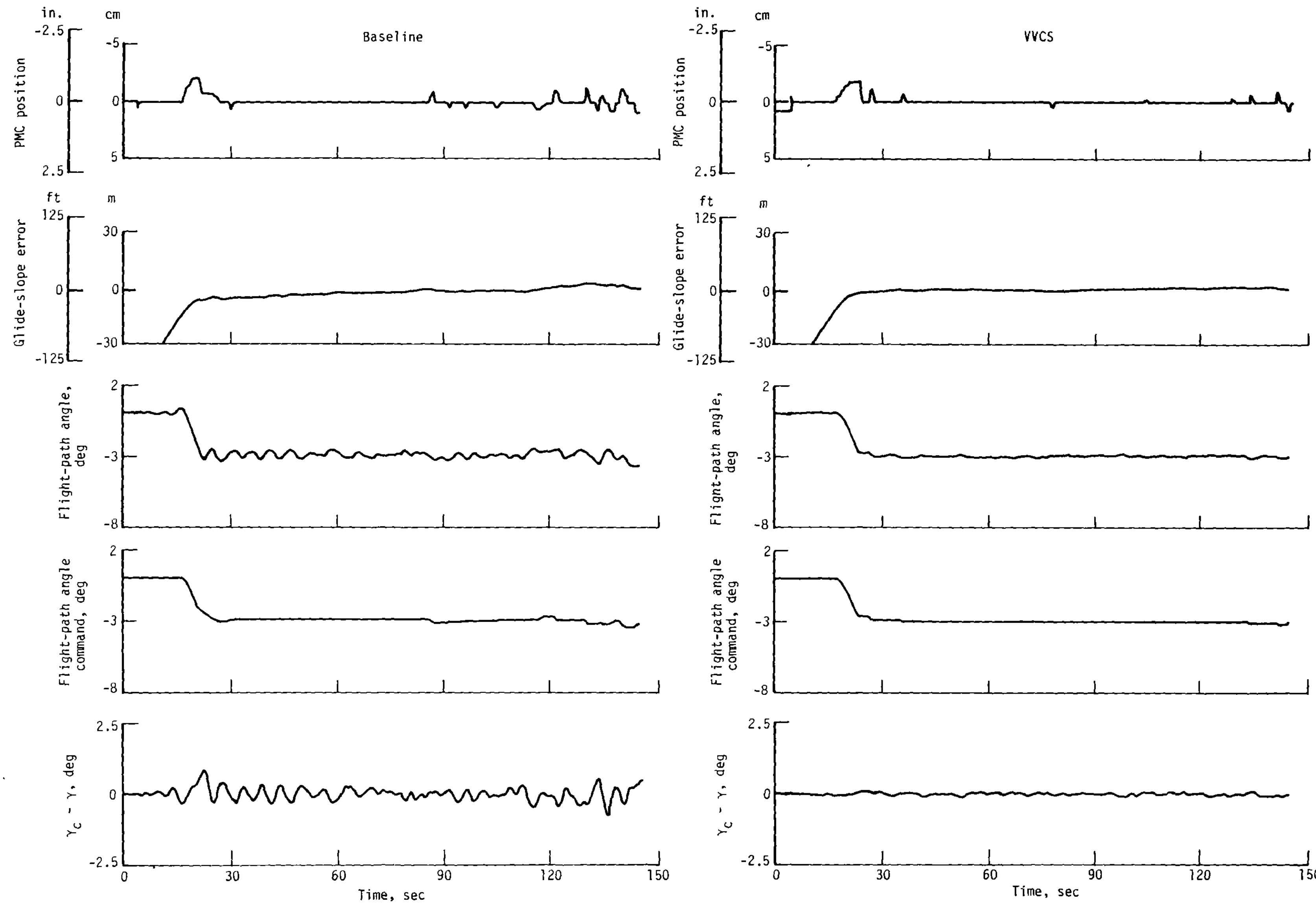

Figure 6.- ILS tracking task data with 10-knot tail wind.

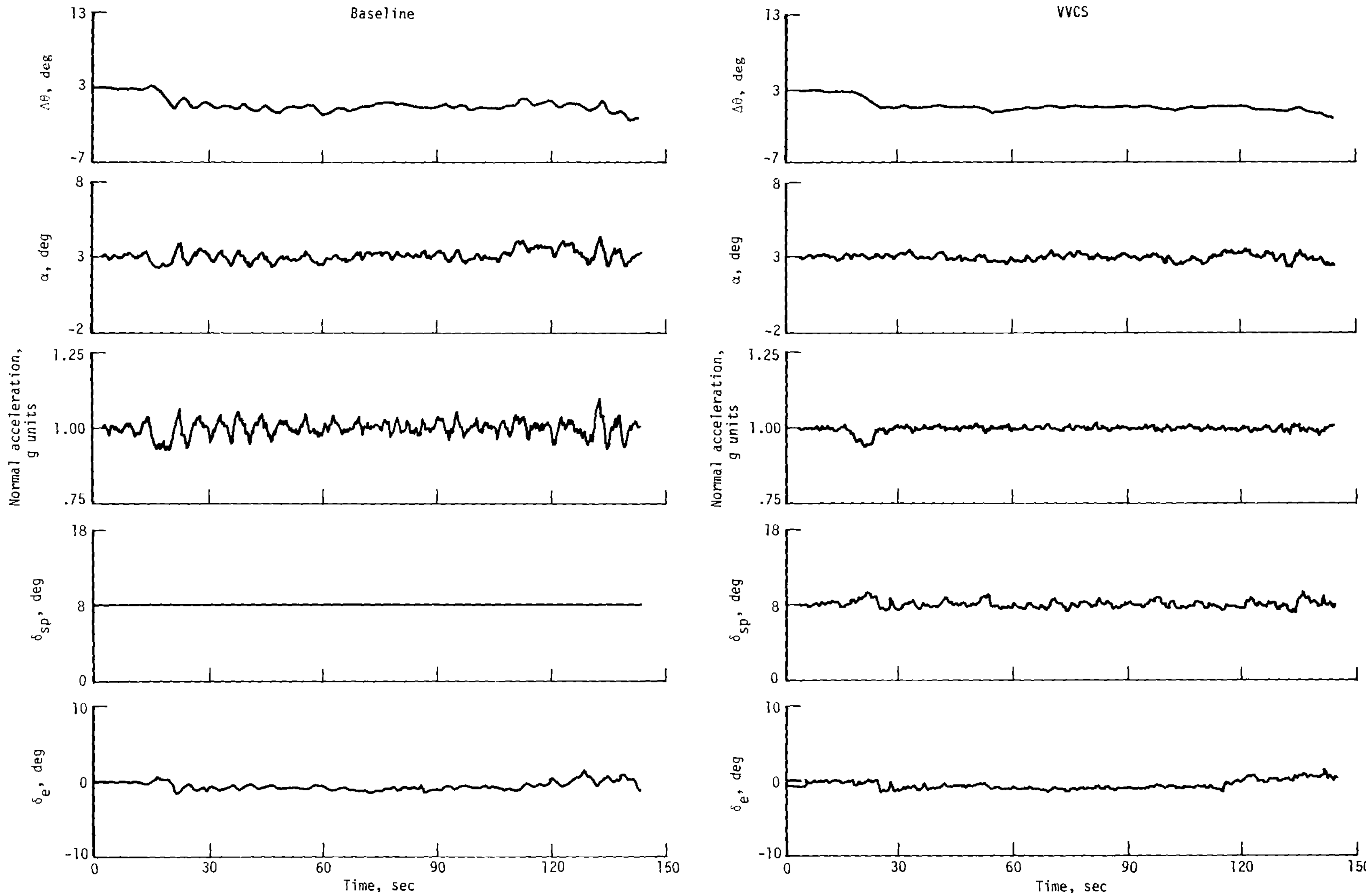

Figure 6.- Concluded.

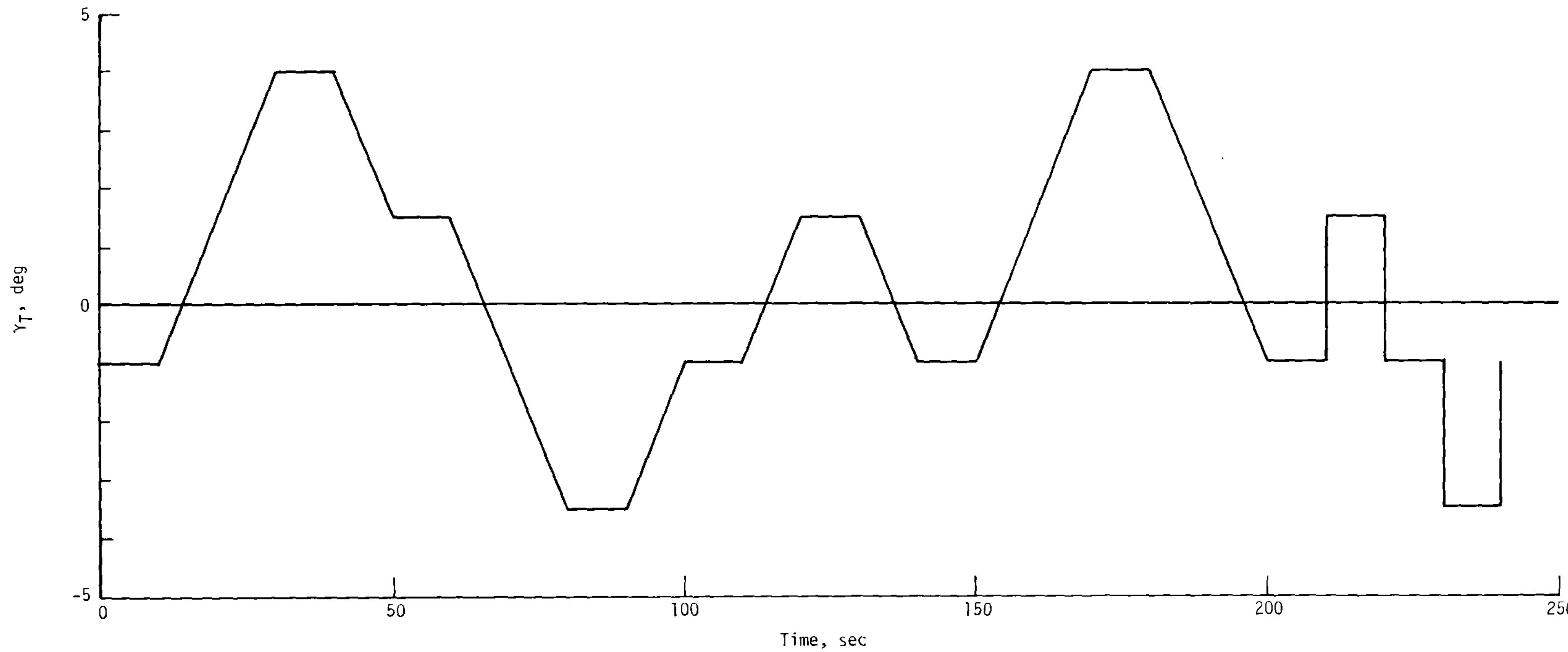

Figure 7.- Flight-path-angle tracking task.

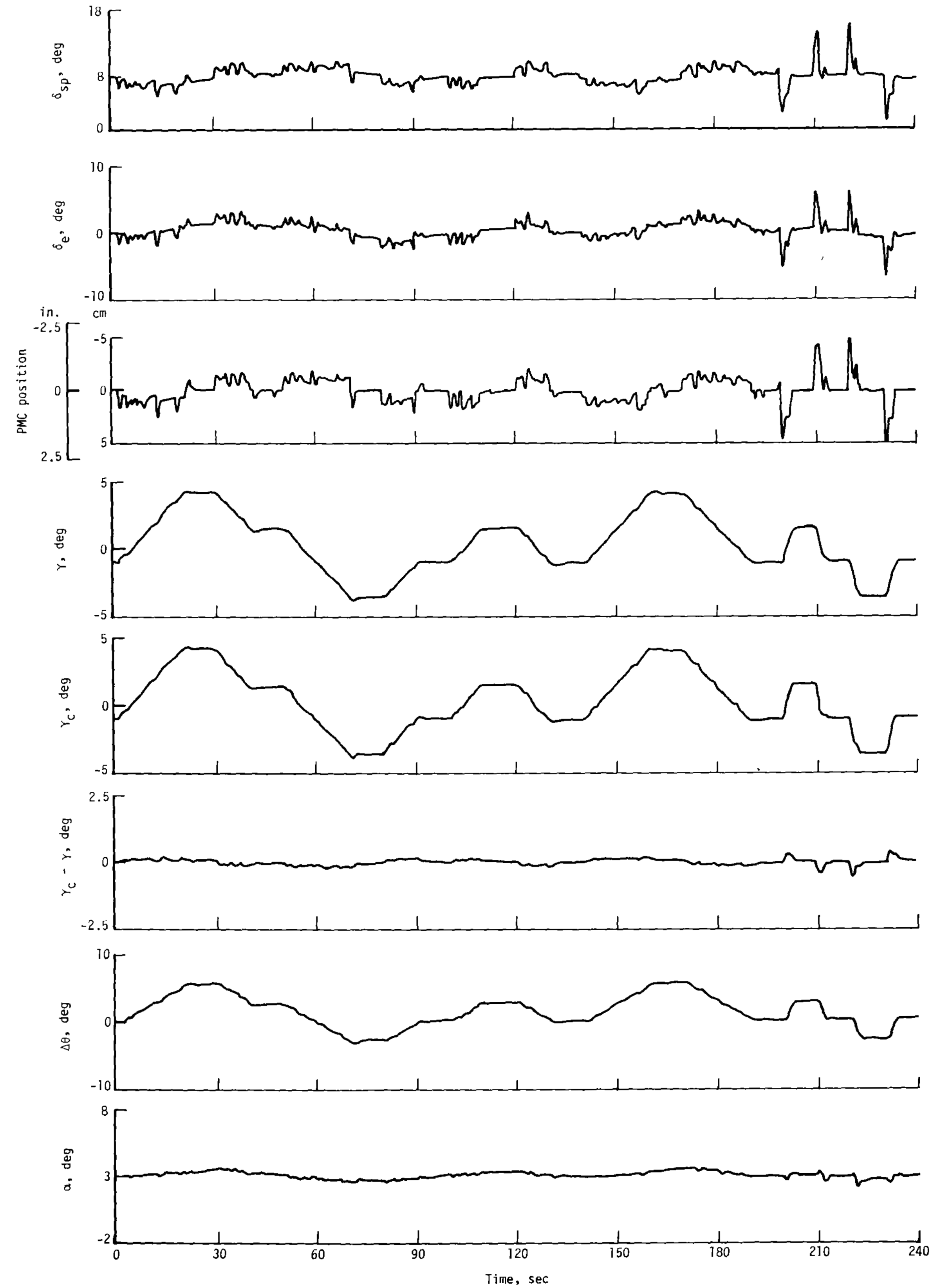

Figure 8.- Flight-path-angle tracking data for VVCS.

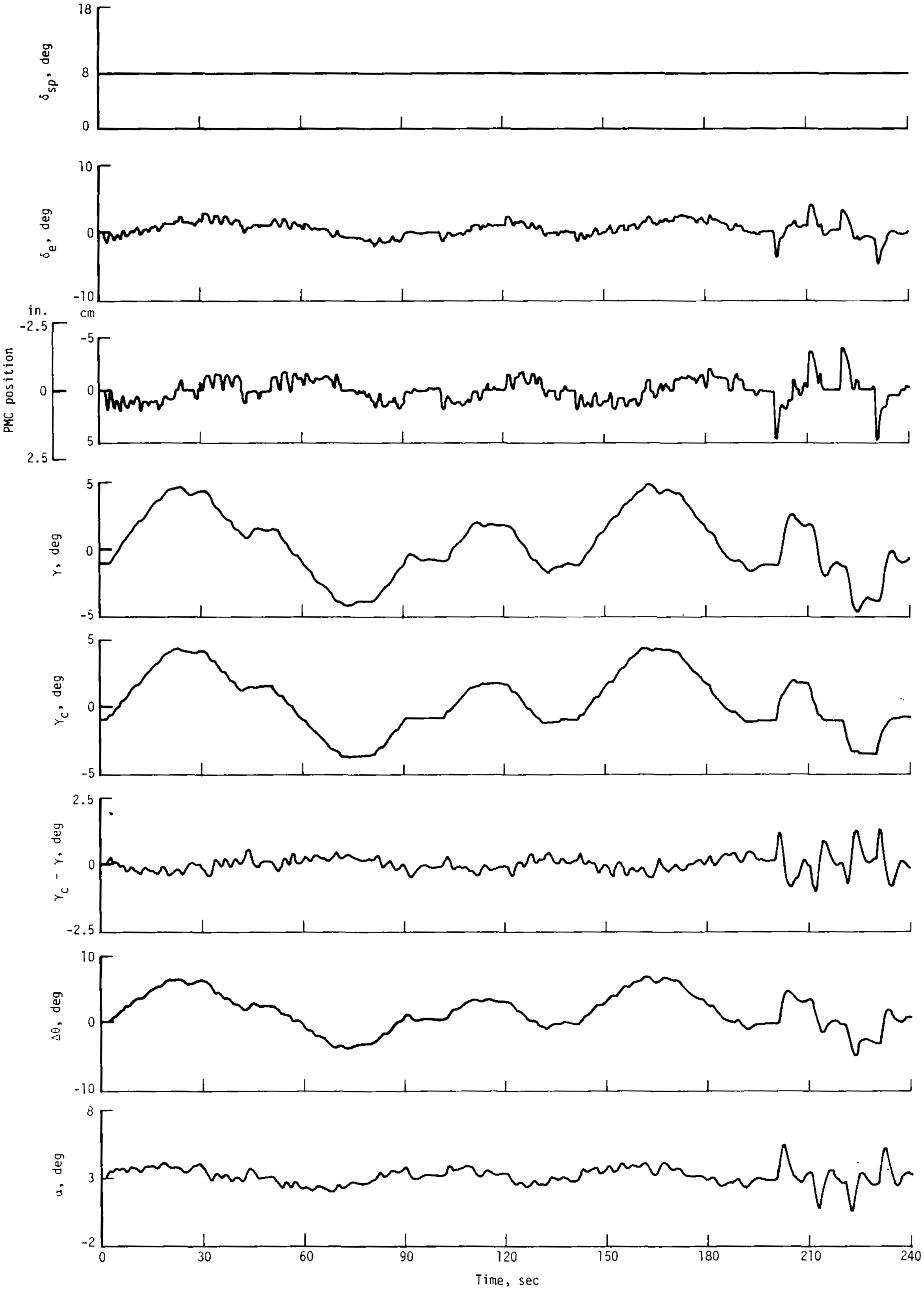

Figure 9.- Flight-path-angle tracking data for baseline system.

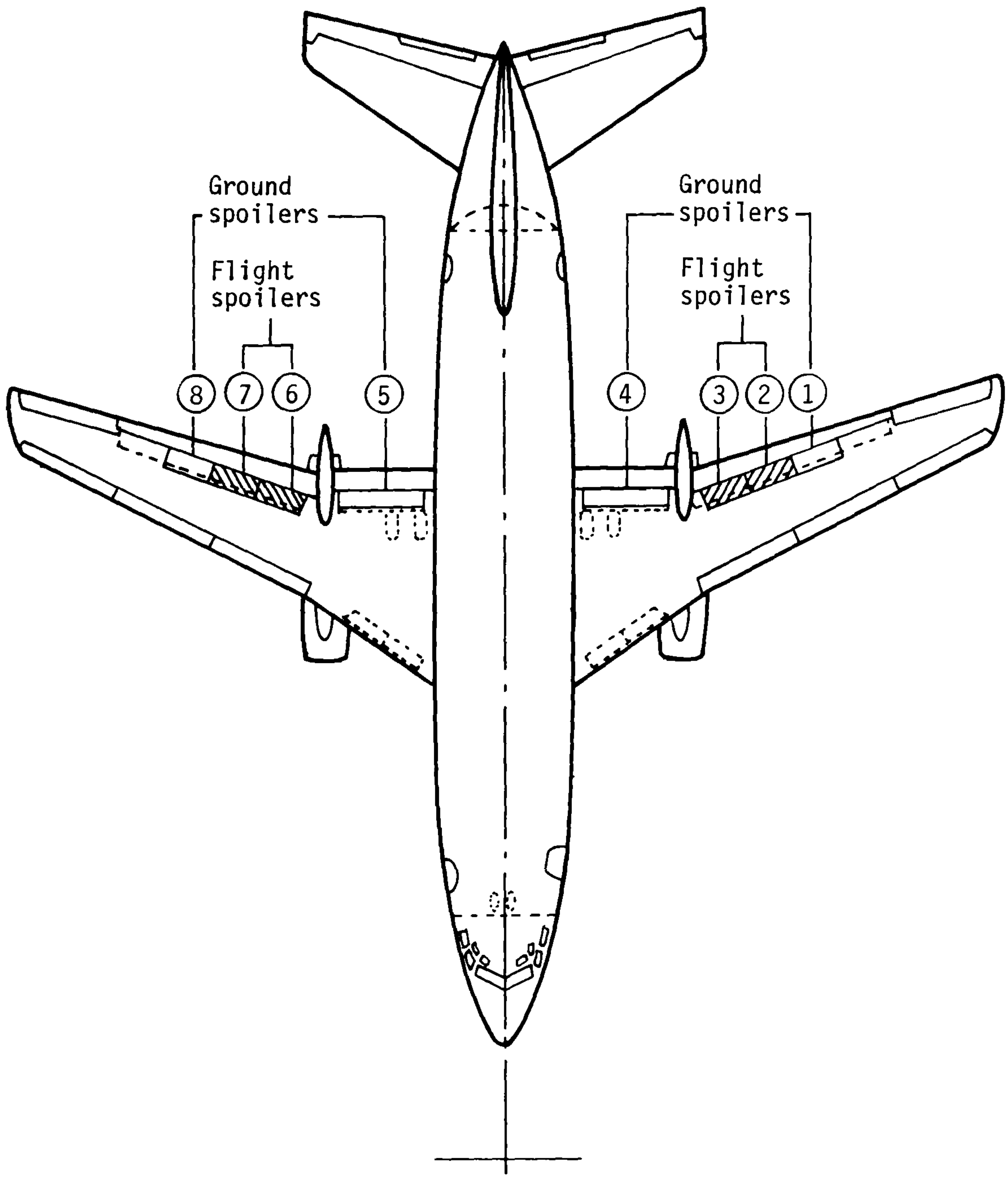

Figure 10.- Spoiler panel identification.

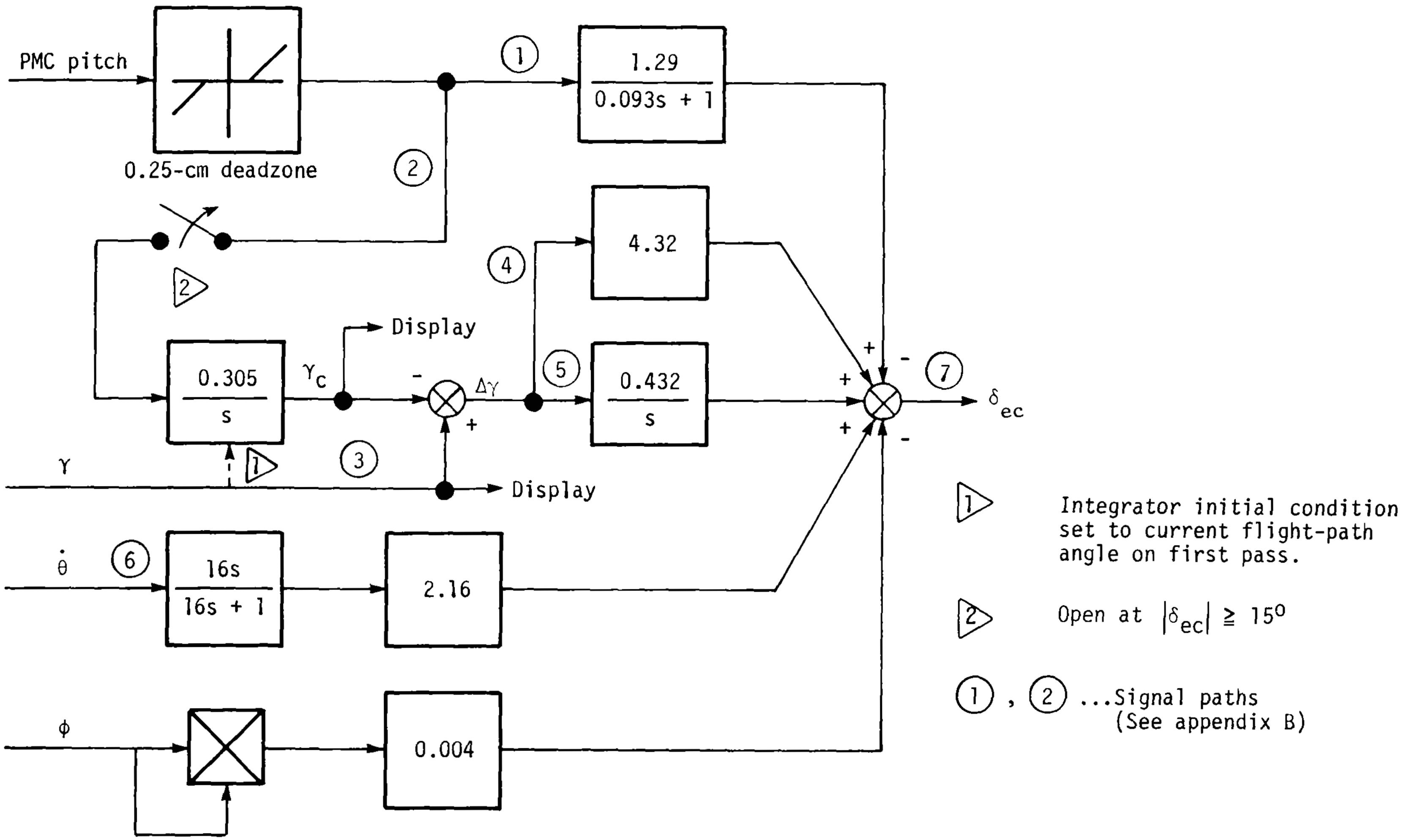

(a) SI units.

Figure 11.- Control law of baseline system.

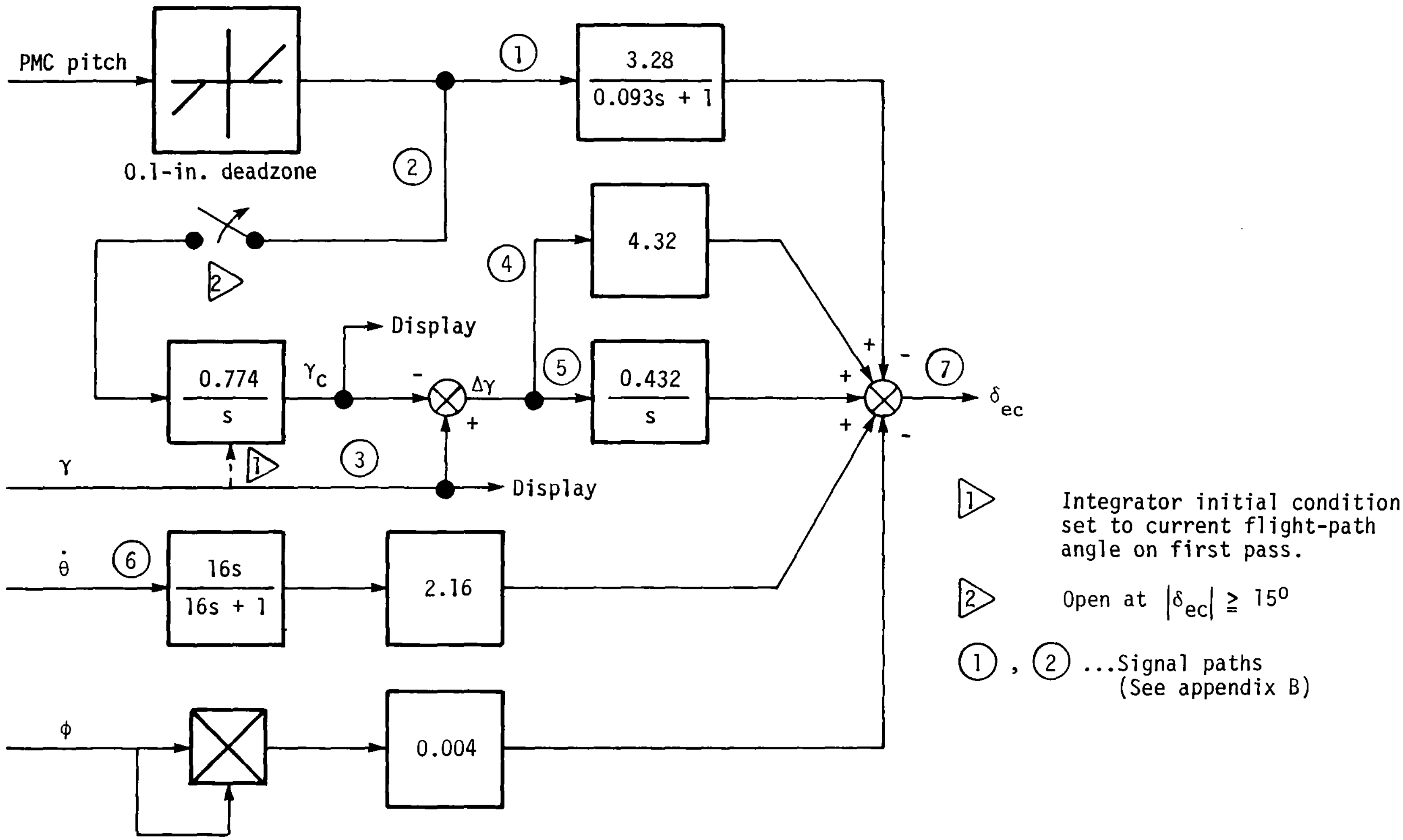

(b) U.S. units.

Figure 11.- Concluded.

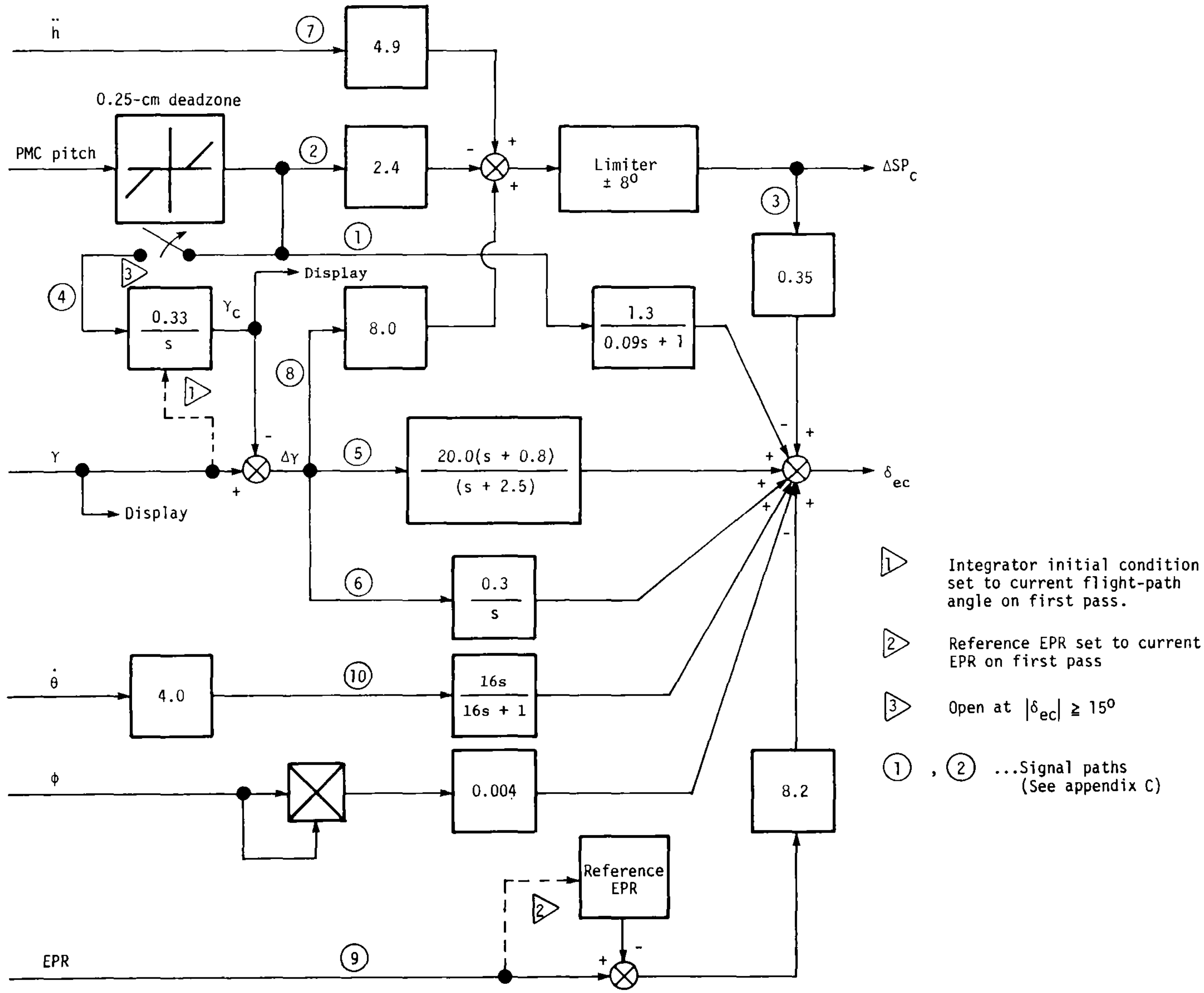

(a) SI units.

Figure 12.- Control law for Velocity Vector Control System.

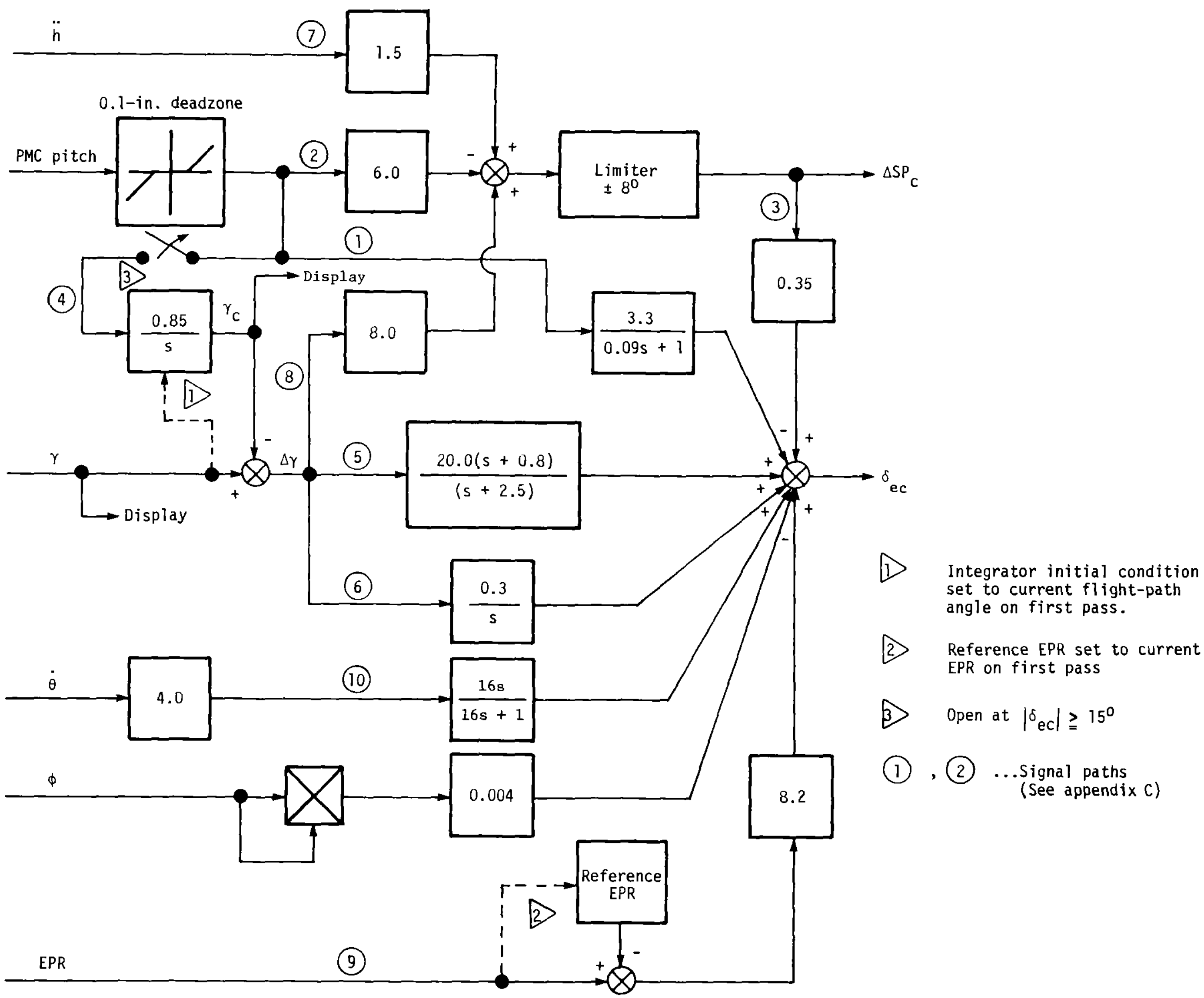

(b) U.S. units.

Figure 12.- Concluded.

1. Report No.	2. Government Accession No.	3. Recipient's Catalog No.
NASA TP-1116		

4. Title and Subtitle
SIMULATOR EVALUATION OF A FLIGHT-PATH-ANGLE CONTROL SYSTEM FOR A TRANSPORT AIRPLANE WITH DIRECT LIFT CONTROL

5. Report Date
March 1978

6. Performing Organization Code

7. Author(s)
Wendell W. Kelley

8. Performing Organization Report No.
L-11947

9. Performing Organization Name and Address
NASA Langley Research Center
Hampton, VA 23665

10. Work Unit No.
513-52-13-52

11. Contract or Grant No.

12. Sponsoring Agency Name and Address
National Aeronautics and Space Administration
Washington, DC 20546

13. Type of Report and Period Covered
Technical Paper

14. Sponsoring Agency Code

15. Supplementary Notes

16. Abstract

A piloted simulator was used to evaluate the flight-path-angle control capabilities of a system that employs spoiler direct lift control. This system was designated the Velocity Vector Control System and was compared with a baseline flight-path-angle control system which used elevator for control. The simulated airplane was a medium jet transport that is used as a research vehicle by the National Aeronautics and Space Administration (NASA). Research pilots flew a manual instrument landing system glide-slope tracking task and a variable flight-path-angle task in the landing configuration to obtain comparative performance data.

17. Key Words (Suggested by Author(s))		18. Distribution Statement
Direct lift controls	Transport airplane	Unclassified - Unlimited
Spoilers	Flight control	
Flight-path angle	Glide paths	
Longitudinal control		Subject Category 08

19. Security Classif. (of this report)	20. Security Classif. (of this page)	21. No. of Pages	22. Price*
Unclassified	Unclassified	30	$4.50

* For sale by the National Technical Information Service, Springfield, Virginia 22161

NASA-Langley, 1978

National Aeronautics and
Space Administration

Washington, D.C.
20546

Official Business
Penalty for Private Use, $300

THIRD-CLASS BULK RATE

Postage and Fees Paid
National Aeronautics and
Space Administration
NASA-451

U.S.MAIL

1 1 1U,A, 021078 S00903DS
DEPT OF THE AIR FORCE
AF WEAPONS LABORATORY
ATTN: TECHNICAL LIBRARY (SUL)
KIRTLAND AFB NM 87117

NASA

POSTMASTER: If Undeliverable (Section 158
Postal Manual) Do Not Return